HFIP Extraction Followed by 2D CTAB/SDS-PAGE Separation: A New Methodology for Protein Identification from Tissue Sections after MALDI Mass Spectrometry Profiling for Personalized Medicine Research

Rémi Longuespée,[1,2] Christophe Tastet,[3] Annie Desmons,[1] Olivier Kerdraon,[1,4] Robert Day,[2] Isabelle Fournier,[1] and Michel Salzet[1]

Abstract

Matrix-assisted laser desorption ionization mass spectrometry imaging (MALDI-MSI) and profiling technology have become the easiest methods for quickly accessing the protein composition of a tissue area. Unfortunately, the demand for the identification of these proteins remains unmet. To overcome this bottleneck, we combined several strategies to identify the proteins detected via MALDI profiling including on-tissue protein extraction using hexafluoroIsopropanol (1,1,1,3,3,3-hexafluoro-2-propanol, HFIP) coupled with two-dimensional cetyl trimethylammonium bromide/sodium dodecyl sulfate–polyacrylamide gel electrophoresis (2D CTAB/SDS-PAGE) for separation followed by trypsin digestion and MALDI-MS analyses for identification. This strategy was compared with an on-tissue bottom-up strategy that we previously developed. The data reflect the complementarity of the approaches. An increase in the number of specific proteins identified has been established. This approach demonstrates the potential of adapted extraction procedures and the combination of parallel identification approaches for personalized medicine applications. The anatomical context provides important insight into identifying biomarkers and may be considered a first step for tissue-based biomarker research, as well as the extemporaneous examination of biopsies during surgery.

Introduction

MATRIX-ASSISTED LASER DESORPTION IONIZATION (MALDI) mass spectrometry profiling and imaging have become valuable tools for histological analyses (Gagnon et al., 2012). Nevertheless, the identification of the detected proteins after MALDI MSI or profiling remains a major bottleneck for this technology. To address this problem, some teams experimented strategies based on the localization of intact proteins provided via MALDI-MSI and the identification of these proteins after their extraction from a consecutive section prior to separation via nano liquid chromatography (LC), and bottom-up analyses (Balluff et al., 2011). In this context, some specific cancer markers have been detected, for example, FXYD3, S100A11, and GSTM3 in

colon cancer (Meding et al., 2012), COX7A2, S100-A10, and TAGLN2 in Barrett's adenocarcinoma (Elsner et al., 2012). This strategy enabled the identification and localization of the highly soluble proteins. Other strategies such as off-tissue analyses have been undertaken. The off-tissue strategy consists of combining MALDI-MSI and LC-MS/MS in a single workflow, thus improving protein identification. The proteins are on-tissue digested, fractionated, and then extracted prior to nano LC separation, followed by MS/MS analysis for databank interrogation (Stauber et al., 2008). This approach was shown to improve protein identification; however, because it is performed on the entire tissue section or half of a tissue section, information about protein localization is lost. A back correlation to the imaging data of tryptic peptides has previously been performed on FFPE tissue samples (Lemaire

[1]Laboratoire de Protéomique, Réponse Inflammatoire, Spectrométrie de Masse (PRISM), MALDI Imaging Team, and [3]Laboratoire de Signalisation des facteurs de croissance dans le cancer du sein—Protéomique Fonctionnelle, Université de Lille 1, Cité Scientifique, Lille, France.
[2]Institut de pharmacologie de Sherbrooke et Département de chirurgie/urologie, Faculté de médecine et des sciences de la santé, Université de Sherbrooke, Sherbrooke, Québec, Canada.
[4]Laboratoire d'Anatomie et de Cytologie Pathologiques, CHRU Lille, Lille Cedex, France.

et al., 2007; Stauber et al., 2008). Recently, newly developed microproteomics methods were proposed, using local micro-extraction using a microjunction extraction procedure (Quanico et al., 2013; Wisztorski et al., 2013). Recently, the combination of the classical approaches of MALDI imaging with bottom-up and top-down proteomics raised to the identification of the classically extracted proteins from fresh/frozen (fr/fr) tissue sections in MALDI imaging experiments. This gave rise to the Matisse database, a publicly available database of the identified proteins in fr/fr tissue sections from MALDI imaging datasets (Maier et al., 2013). This method is fully applicable to the classically performed MALDI analyses but it still remained an unmet need for high-mass and hydrophobic proteins.

We developed two complementary strategies for identifying specific proteins and performing back correlations to the MALDI profiling data obtained after procedures for high-mass protein extraction. We integrated local on-tissue digestion followed by tissue extraction and separation via nano LC and ESI-MS analysis with a method for the extraction of higher mass proteins directly on the tissues using HFIP (1,1,1,3,3,3-hexafluoro-2-propanol). We previously demonstrated that a HFIP solution allowed for the extraction of both high-mass proteins (Franck et al., 2010; van Remoortere et al., 2010) and low-mass proteins (Longuespee et al., 2012a) from fr/fr tissues. This procedure facilitated access to rat brain section proteins measuring up to 70 kDa, and the visualization of these proteins in MALDI MSI (Franck et al., 2010; van Remoortere et al., 2010). Prior to these HFIP developments, MALDI profiling and MSI were limited to the detection of proteins less than 30 kDa. This represented a real methodological limitation because many classes of proteins with important biological activities, such as most enzymes, receptors, pro-proteins, and neuropeptide precursors, are larger than 25 kDa.

In another study, we were able to detect proteins of up to 100 kDa with a dramatically increased signal/noise ratio (van Remoortere et al., 2010). Although this method was applicable to the determination of high-mass protein molecular features from ovarian cancer samples (El Ayed et al., 2010), the identification of these proteins remained an important issue in this investigation because the MALDI TOF instrumentation does not allow us to fragment the detected native proteins. New methods have been proposed for the identification of on-tissue proteins using a combination of these treatments and In Source Decay (ISD) fragmentation (Calligaris et al., 2013). Currently, there is a challenge in both detecting and identifying a variety of proteins on tissue sections.

Here, we applied a new method for protein extraction from tissue slices based on HFIP high-mass protein extraction combined with 2D CTAB/SDS-PAGE separation and MALDI time of flight–time of flight (TOF-TOF) identification. We then combined the data obtained by this strategy with the data obtained via on-tissue digestion, micro-extraction, and shot-gun analyses. The combination of the two strategies results in improved protein identification. This development (applied here for ovarian cancer) may be used for a variety of other diseases.

Materials and Methods

Sinapinic acid (SA), 1,1,1,3,3,3-hexafluoro-2-propanol (HFIP), trifluoroacetic acid (TFA), pyronin Y, acrylamide/ N,N'-methylenebisacrylamide, acetone, acetonitrile (ACN), chloroform, and Water Chromasolv Plus for HPLC (H_2O) were purchased from Sigma-Aldrich (Saint Quentin Fallavier, France).

Samples of ovarian biopsies

Tissues (fr/fr and FFPE) were obtained from the CHRU de Lille pathology department. An institutional review approval (CPP Nord Ouest IV 12/10) was obtained. Patient information, including, age, treatment received prior to and after surgery, extent of surgery, current status (alive, alive with progressive disease, deceased, and cause of death), and survival from the time of original pathologic diagnosis were collected. The International Federation of Gynecology and Obstetrics (FIGO) stages for each specimen were determined, and the results of the histological examinations were recorded.

Tissue preparation of ovarian biopsies

Thin 10- to 12-μm fr/fr tissue sections were cut from frozen ovarian biopsies using a Leica CM1510S cryostat (Leica Microsystems, Nanterre, France) and placed onto ITO-coated conductive glass slides (Bruker Daltonics, Bremen, Germany). For the ovarian biopsies from adjacent hematoxylin eosin safran (HES)-stained sections, the histopathologic diagnoses were performed by a pathologist (OK) who was blinded to the original clinical diagnosis. The tissue sections were submitted to different washing steps to remove salts and abundant lipids. Each tissue section was first immersed in a bath of cold acetone for 30 sec, followed by a bath of cold EtOH 95% for 30 sec and finally immersed in chloroform for 1 min (Lemaire et al., 2006).

Mass spectroscopy methods

HFIP extraction method.   To extract the compounds from the small tissue area biopsies, a hydrophobic solvent was used following the procedure previously described by our group (Franck et al., 2010; Longuespee et al., 2012a; van Remoortere et al., 2010). A total of 10 mg of SA was dissolved in 1 mL HFIP. A total of 3 μL of the solution was manually dropped onto the region of interest in six 0.5 μL droplets using gel loader tips. After this deposition, 3 μL of 10 mg/mL SA in 1% ACN/aqueous TFA (7:3) was added.

Tissue profiling using MALDI mass spectrometry.   The molecular profiling was performed on an UltraFlex II MALDI-TOF/TOF instrument (Bruker Daltonics) equipped with a micro-channel plate (MCP) detector. The instrument was equipped with a Smartbeam[TM] laser and was controlled using FlexControl 3.0 (Build 158) software (Bruker Daltonics). For the stage I tissue biopsies, the raw spectra were compared using FlexAnalysis 3.0 (Bruker Daltonics). Spectra from ovarian cancer biopsies were analyzed with FlexAnalysis 3.0 (Bruker Daltonics). The mass spectrometry imaging datasets were recorded in positive ion and linear time-of-flight modes and averaged 1000 laser shots for each position. The analysis of the higher mass proteins required higher laser fluencies. Typically, for these experiments, the laser offset was set to 30%, laser range 20%, laser fluence 70%, and the laser focus was set to medium.

Intact protein extraction and identification

2D CTAB/SDS-PAGE analyses. For the 2D PAGE analysis, we collected 10 tissue sections, each of a 10 μM thickness. We alternatively dropped each tissue section into separate tubes for the study. This type of sampling enables a representative repartition of the global protein content of the tissue in each tube. For the solvent extraction comparison experiments, we dropped 1 mL of the solution of ACN/TFA0.1%aq 7:3 into one tube. In parallel, we dropped 1 mL of HFIP in another tube. We then solubilized the preparations via vortexing until the tissue sections in the HFIP tube were totally solubilized. After solubilization, a lipid supernatant is visible at the top of the preparation in the HFIP tube; this supernatant was removed. In the ACN/TFA0.1%aq preparation, a tissue pellet remained, and the supernatant was kept for analysis after a 13,000 *g* centrifugation. Only the solubilized compounds in each preparation were kept for analysis when using these preparations.

The HFIP and ACN/TFA0.1% aq extract were evaporated via freeze drying using a SpeedVac (Savant) prior to separation in 2D gel electrophoresis. The hydrophobic proteins were resolved via 2-DE using cationic CTAB-polyacrylamide gels (CTAB-PAGE: 16×20 cm, 0.75 mm thickness) in the first dimension and conventional SDS-polyacrylamide gels (SDS-PAGE: 18×20 cm and 1.5 mm thickness) in the second dimension. All protein separations were performed at 11°C using the Protean II XL electrophoresis system (Bio-Rad, Hercules, CA, USA). Each tissue sample was mixed with 100 μL of loading buffer (3 M urea, 2% w/v CTAB, 50 mM DTT, 10% v/v glycerol, 100 mM phosphate buffer pH 3, and 0.05% of pyronin Y as tracking dye), sonicated on ice (Bandelin Sonopuls HD 2200 with a titanium microtip MS 72, Berlin, Germany) for 4×10 sec (power 10%) and centrifuged at 10,000 *g* at room temperature for 15 min to remove the insoluble material. For CTAB-PAGE, discontinuous slab gels consisting of a 4% stacking gel [4% w/v acrylamide/N,N'-methylenebisacrylamide solution (29:1), 3 M urea, 0.1% w/v CTAB, 0.1 M phosphate buffer pH 3] and a 6% resolving gel [6% w/v acrylamide/N,N'-methylenebisacrylamide solution (29:1), 3 M urea, 0.1% w/v CTAB, 0.1 M NaOH, 0.2 M orthophosphoric acid] were used. Due to the acidic pH conditions, the gels were photopolymerized for 1 hour using a methylene blue-based system (Lyubimova et al., 1993). The cationic gels were electrophoresed overnight at a constant voltage of 100 V and a reversed polarity compared with SDS-PAGE in a running buffer consisting of 25 mM orthophosphoric acid, 150 mM glycine, and 0.1% w/v CTAB until the tracking dye reached the bottom edge of the resolving gel. The loading empty lanes in comparable volumes with 5 μg cytochrome C from bovine heart (Sigma-Aldrich, St. Louis, MO, USA) circumvented the gel distortions. After first dimension migration, the CTAB gels were cut into strips of 1 cm and equilibrated twice for 30 min in 2.5% (w/v) SDS, 0.125 M 1-thioglycerol, 20% v/v glycerol, and 0.125 M Tris-HCl pH 6.8. The excised lanes were then transferred on conventional Laemmli-10% SDS-PAGE for the second-dimension electrophoresis. The SDS-PAGE were carried out with an electrode buffer consisting of 192 mM glycine, 25 mM Tris, 0.1% w/v SDS, and at pH 8.3 at a constant current of 20 mA/gel in the stacking phase, followed by 35 mA/gel in the resolving phase until the bromophenol blue

dye reached the bottom of the gels. Protein detection was achieved using Biosafe Coomassie staining (Bio-Rad).

Trypsin digestion of the 2D CTAB/SDS-PAGE spots

The gels were then washed in water for 2 additional days. Spots of interest were then cut and rinsed with 100 μL ammonium bicarbonate buffer 50 mM (pH 8)/ acetonitrile 80% to remove the Coomassie Blue. The gel fragments were then incubated overnight with 50 μL of 50 mM trypsin. After vortexing, the supernatant was kept, and 100 μL ACN/Water 1:1 v:v were added to the gel fragments. After vortexing, the supernatant was then recovered and mixed with the first supernatant. The solution was then dried with a SpeedVac, and the peptides were taken in 20 μL of pure water.

Bottom-up strategy

MALDI mass spectrometry profiling methodology. For each tissue, 50 spectra were acquired on spots homogeneously distributed across the analysis surface. The profiles were acquired using an UltraFlex II MALDI-TOF/TOF instrument (Bruker Daltonics) equipped with a smart beam laser with a 200 Hz repetition rate and controlled by Flex-Control 2.5 software (Bruker Daltonics). The mass spectra profiles were acquired in the positive reflection mode in the 500–5500 Da mass ranges. One thousand spectra were acquired at each position using a 200 Hz laser frequency.

Antigen retrieval and trypsin digestion. FFPE tissues were treated by citric acid antigen retrieval, as previously described (Longuespee et al., 2013b).

Ten milliliters in total of a solution containing 40 mM trypsin in 50 mM ammonium bicarbonate were dropped onto each discrete tissue region of interest using gel loader tips (the 10 microliters were dropped 5 times using 2 microliters of solution). This procedure prevents the drop from spreading and thus to have a mix up of different cell types digests. The slides were then incubated for 4 h at 37°C in a customized humidity chamber (a 10 cm × 15 cm box filled with water to one-quarter of the box height and placed in a 37°C incubator). After trypsin digestion, 10 μL of a 10 mg/mL HCCA solution in aqueous TFA 0.1%/ACN (3:7) was dropped onto each section

Principal component analysis. The data were obtained using FlexImaging II 2.5 software (Bruker Daltonics) and loaded into the ClinProTools v2.5 software (Bruker Daltonics) to conduct the principal component analysis (PCA) and hierarchical clustering analysis. After the standardization of the data, the unsupervised PCA method was selected. The PC1 and PC2 components were found to have the largest variance (Bonnel et al., 2011; Deininger et al., 2008).

LC MS/MS analyses. Trypsin-digested peptides were manually extracted from specific tissue regions after PCA. Using a micropipette, specific regions were subjected to 20 successive washes with 100 μL of 80% ACN in water. The extract solution was then dried with a SpeedVac (Savent). The dried peptides were re-dissolved in 10 μL 0.1% TFA. The salts were removed from the solution, and peptides were concentrated using a solid-phase extraction procedure with a Millipore ZipTip device in 10 μL 80% ACN elution solution. The solution was dried again using a SpeedVac, and the dried

samples were resuspended in a solution of 5% acetonitrile and 0.1% formic acid. The samples were separated via online reversed-phase chromatography using a Thermo Scientific Proxeon Easy-nLC system equipped with a Proxeon trap column (100 μm ID$\times$2 cm, Thermo Scientific) and a C18 packed-tip column (100 μm ID$\times$15 cm, Nikkyo Technos Co. Ltd). The peptides were separated using an increasing concentration of acetonitrile (5%–40% over 110 min) at a 300 nL/min flow rate. The LC eluent was electrosprayed directly from the analytical column, and a 1.7 kV voltage was applied via the liquid junction of the nanospray source. The chromatography system was coupled to a Thermo Scientific Orbitrap Elite mass spectrometer, which was programmed to acquire in a data-dependent mode. The survey scans were acquired in the Orbitrap mass analyzer operating at a 120,000 (FWHM) resolving power. A mass range of 400 to 2,000 m/z and a target of 1E6 ions were used for the survey scans. The precursors observed with an intensity of over 500 counts were selected ''on the fly'' for the ion trap collision-induced dissociation (CID) fragmentation with an isolation window of 2 amu and a normalized collision energy of 35%. A target of 5000 ions and a maximum injection time of 200 ms were used for the CID MS^2 spectra. The method was set to analyze the twenty most intense ions from the survey scan, and a dynamic exclusion was enabled for 20 sec. Each sample was analyzed three times. The limit of detection of the instrumentation is 25,000 peptides for an LC-MS/MS run.

Databanks analysis

The tandem mass spectra were processed using the Thermo Scientific Proteome Discoverer software version 1.3. The resultant spectra were matched against the Swiss-Prot® Human database (version January 2012) using the SEQUEST® algorithm. The search was performed by selecting trypsin as the enzyme with two missed cleavages allowed. The precursor mass tolerance was 10 ppm, and the fragment mass tolerance was 0.5 Da. N-terminal acetylation, methionine oxidation, and arginine deamination were set as the variable modifications. A peptide validation was performed using the Percolator algorithm. The peptides were filtered based on a q-value of 0.01, which corresponds to a 1% false discovery rate (FDR).
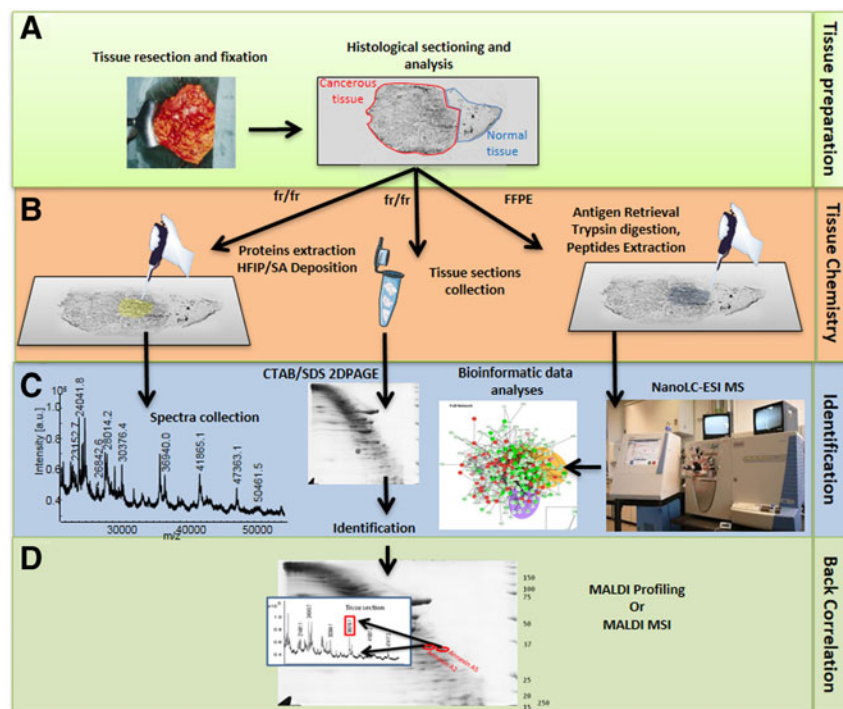
Only proteins with a score of over 5, which represents the proteins identified with two or more unique peptides, were kept for analysis. The relative protein expression was calculated based on the protein score, which was shown to be an adequate relative indicator of the relative differential expression (Colinge et al., 2005; Nanduri et al., 2005).
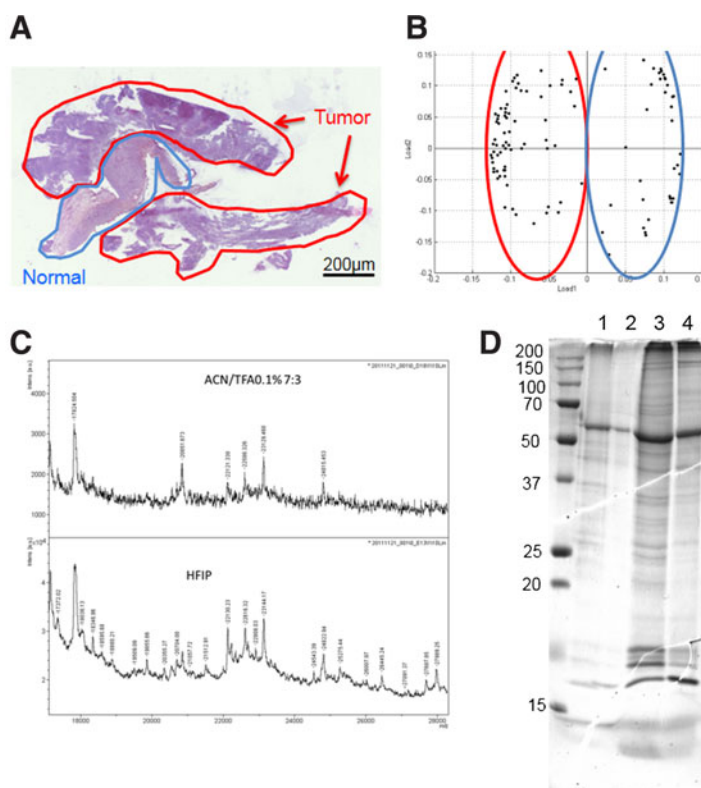
Results

The global workflow of the methodology is illustrated in Figure 1. We sought to combine the advantages of new proteins extraction procedures from tissues for both MALDI profiling with the already described procedures (Franck et al., 2010; van Remoortere et al., 2010) and the identification of the detected protein via 2D gel electrophoresis. These results were then compared with those obtained with on tissue digestion and shotgun analyses.

Solvent-based tissue solubilization evaluation

To evaluate the solubilization efficiency of different solvent mixes for the on-tissue profiling, we compared the amount of proteins observed via 2D electrophoresis after protein solubilization with different mixtures applied on serous ovarian cancer tissue slices (Fig. 2). Prior to solvent

FIG. 1. Scheme of the strategy used to localize (via MALDI MS profiling) the high mass proteins, extract them, identify them, and perform the back correlation.

FIG. 2. **(A)** Ovarian cancer tissue section stained with hematoxylin eosin safran (HES) and annotated by the pathologist. **(B)** MALDI profiling analyses using HFIP/sinapinic acid procedure for high mass protein identification according to (Longuespee et al., 2012a). **(C)** Principal component analyses of the tissue section. **(D)** MALDI MS analyses for extracted proteins with either ACN/TFAaq or HFIP. **(E)** SDS-PAGE analyses of the extracted protein with either ACN/TFAaq (*lanes 1 and 2*) or HFIP (*lanes 3 or 4*).

extraction, tissue sections of serous ovarian cancer (Fig. 2A and 2C) were submitted to MALDI profiling followed by principal component analyses (Fig. 2B) to identify the specific m/z for the cancerous part of the tissue. Twenty tissue sections were then analyzed in the same conditions before being subjected to HFIP or ACN/TFA0.1%aq extraction (10 per conditions). The results show that fewer proteins can be extracted with ACN/TFA0.1% aq solution than with HFIP, in which more proteins are detected with a better signal intensity (Fig. 2C). The collected samples were then dried before being subjected to the 2D gel analyses. However, in the HFIP-extracted sample, the remaining lipid pellet stayed at the top of the gel electrophoresis well and was excluded from the gel separation.

Diagonal poly acrylamide gel electrophoresis method was used for proteins separation, with the anionic SDS and the cationic CTAB detergents- (Braun et al., 2007; Polati et al., 2009; Yamaguchi et al., 2008a, b). A comparison between the HFIP and ACN/TFA0.1% aq extraction procedures was first performed in 1D SDS-PAGE (Fig. 2D). Unequivocally, the amount of protein in the gel from the HFIP-extracted sample (Fig. 2D lanes 3 and 4) was significantly higher than that obtained with the ACN/TFA0.1% aq extraction sample (Fig. 2D lanes 1 and 2). We thus decided to use the HFIP extraction procedure for 2D CTAB/SDS-PAGE separation (Fig. 3) and further analysis. However, a 2D CTAB/SDS-PAGE obtained with ACN/TFA0.1% was obtained and is presented in Supplementary Figure S1 (supplementary material is available online at www.liebertpub.com).
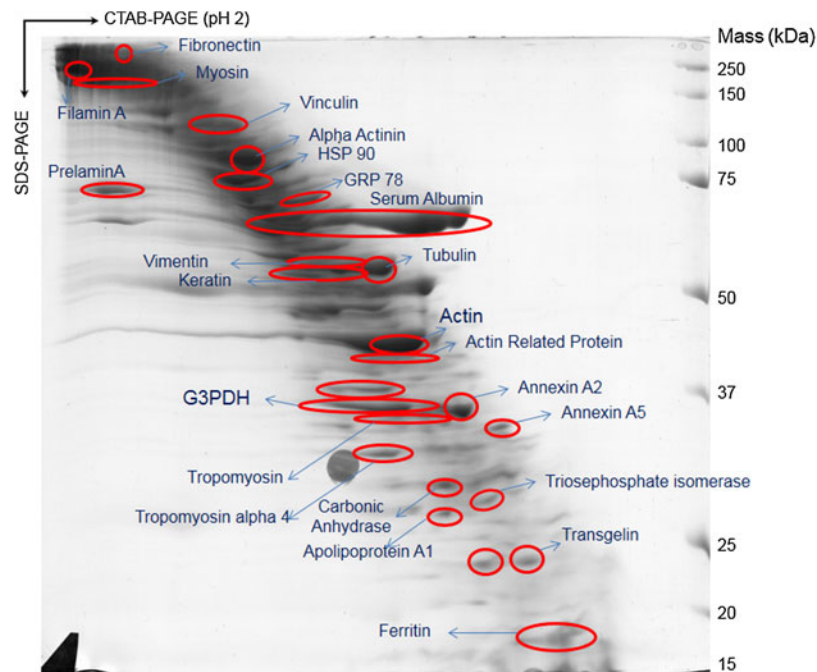
Protein identifications from 2D CTAB/SDS-PAGE spots

The proteins separated in 2D CTAB/SDS-PAGE after the HFIP extractions were subjected to identification. Tryptic digestion was performed for areas of interest prior to identification via peptide mass fingerprint of the selected proteins. It is noteworthy that large sample amounts have to be loaded in the gel to identify the major protein present in a selected spot. In Figure 3, the potential markers of the tissue have been framed, and some of these are classified in Table 1. Among the identified markers in the electrophoresis gel, we focused our attention on annexins. We identified annexin A2 and annexin 5. Annexin 2 is known to be involved in many aspects of ovarian cancer progression and mechanisms associated with metastasis such as cytoskeleton remodeling, cell migration and adhesion, and the mediation of the activation of plasminogen (an enzyme involved in cancer progression) (Lokman et al., 2011). Annexin A2 is also involved in cell proliferation. We also identified annexin A5 (Dong et al., 2009; Rao et al., 1992; Sugimura et al., 1994; Xue et al., 2007). Prelamin A has also been detected. Recent transcriptomic experiments demonstrated an increased expression of lamins A and C in ovarian cancer (Prokocimer et al., 2009), which is in line with our results. Transgelin is a protein associated with the cell migration and adhesion phenomena (Longuespee et al., 2012b), and vinculin is associated with tumor progression. Chaperon proteins (HSP90 and GRP78) have also been characterized. Iron storage is also represented by the discovery of ferritin in the gel spots.

Specific enzymes have also been identified. We identified carbonic anhydrase, which is involved in cell proliferation and adhesion, pH regulation, and intercellular communication. The triose phosphate isomerase is with three other glycoproteins (gp96, palmitoyl-protein thioesterase 1 precursor, and ER-associated DNAJ) upregulated in ovarian cancer and has been specifically detected in paclitaxel resistance tumors (Di Michele et al., 2010). Myosin 9 appears to be involved in the dissemination of ovarian tumors via the

FIG. 3. 2D CTAB/SDS-PAGE of serous ovarian cancer stage I after hexafluoroisopropanol (1,1,1,3,3,3-hexaluoro-2-propanol) extraction on tissue extraction. The proteins identified after spot trypsin digestion and mass spectrometry analyses via MALDI TOF are represented.

implantation of cancer spheroids into the mesothelial monolayer on the walls of peritoneal and pleural cavity organs (Iwanicki et al., 2012). Ovarian tumor cell clusters gain access to the submesothelial environment by exerting force on the mesothelial cells lining the target organs, as well as by driving the migration and clearance of the mesothelial cells (Iwanicki et al., 2012). Finally, in the ovarian tumor, we detected the TRIO and F-actin-binding protein, which is under the regulation of the oncogene c-Myc that is known to stimulate proliferation, sustain tumor maintenance, and modulate cell migration (Pocsfalvi et al., 2011).

Correlation between the proteins identified via 2D CTAB/SDS-PAGE and those identified via shot-gun analyses

For the shot-gun proteomics analyses, trypsin on-tissue peptide digestion from healthy and serous carcinoma ovaries were performed, and the digested peptides were subsequently extracted from the tissue before being subjected to LC MS/MS analyses using Orbitrap Elite. Among the identified proteins, those with a score of less than 5 were removed for subsequent analyses for comparison with those obtained after the HFIP/ 2D CTAB/SDS-PAGE strategy (Table 1). In this context, none of the proteins identified from electrophoresis have been identified in the top scores of the shot-gun analyses, demonstrating that a different panel of proteins is identified with on-tissue bottom-up analyses. Trypsin digests the more accessible proteins and not those present in the membrane or that are highly hydrophobic due to their conformation. Moreover, network analyses using String software confirmed that all proteins identified after HFIP solvent extraction are known to be correlated with each other (Fig. 4A), whereas only a few of those identified using bottom-up strategy are known to be correlated (Fig. 4B).
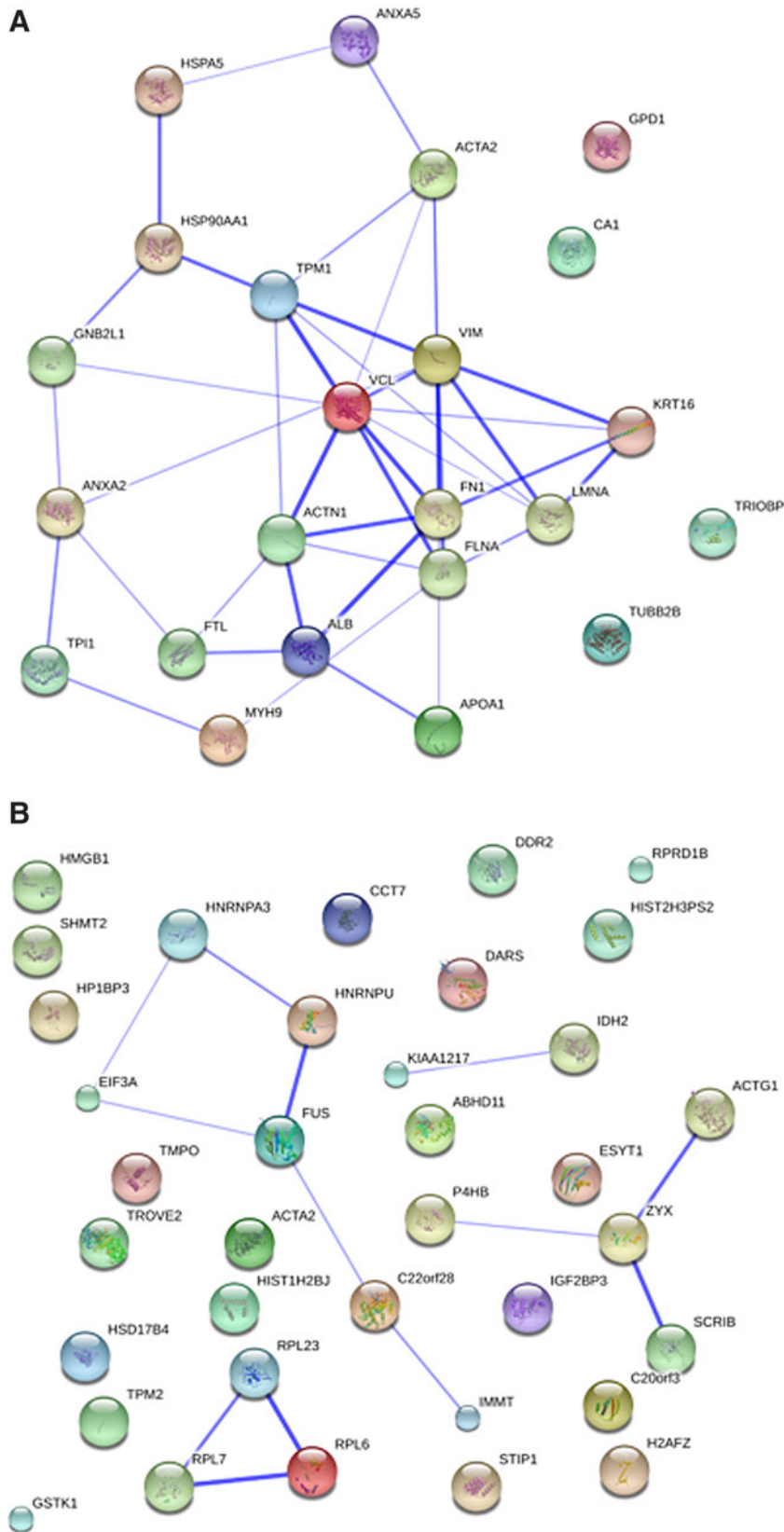
Back correlation to MALDI profiling

Back correlation to the proteins detected via MALDI-TOF profiling is difficult due to the low spectral resolution and mass accuracy of the TOF analyzer. Nevertheless, an attempt was made to back correlate from the proteins identified from the combination of the two strategies and those detected via MALDI profiling after the high-mass procedure. A tissue profiling method for high-mass proteins was performed on serous ovarian cancer biopsies as we previously described (Franck et al., 2010; van Remoortere et al., 2010). A principal component analysis was performed on the carcinoma and healthy regions (Fig. 2C). Based on our own tissues proteomic studies (Table 1), the detection of several of these biomarkers has been predicted (Fig. 5). Thus, proteins with m/z between 20,000 and 50,000 have been attributed via the MALDI MS profile to serous ovarian cancer tissue (Fig. 5). Based on a Protein Atlas Database (ww.proteinatlas.org/search) search, we found that most of these proteins are not detected in immunocytochemistry in ovarian cancer [such as Carbonic anhydrase 1 (CAH1_ HUMAN), Triosephosphate isomerase (TPIS_HUMAN), Annexin A5 (ANXA5_HUMAN), and Annexin A2 (ANXA2_ HUMAN)]. However, most of the results were dependent on the antibody used.

The proteins ranged from 20,000 to 50,000 m/z. Some had already been identified in patients' serum. Triosephosphate isomerase (TPI) is a marker for multidrug resistance in neoplastic (Di Michele et al., 2010) or damaged cells. Carbonic anhydrase 1 was also detected in ovarian tumors. This

TABLE 1. SEROUS OVARIAN CANCER PROTEINS IDENTIFIED AFTER EITHER ON-TISSUE DIGESTION
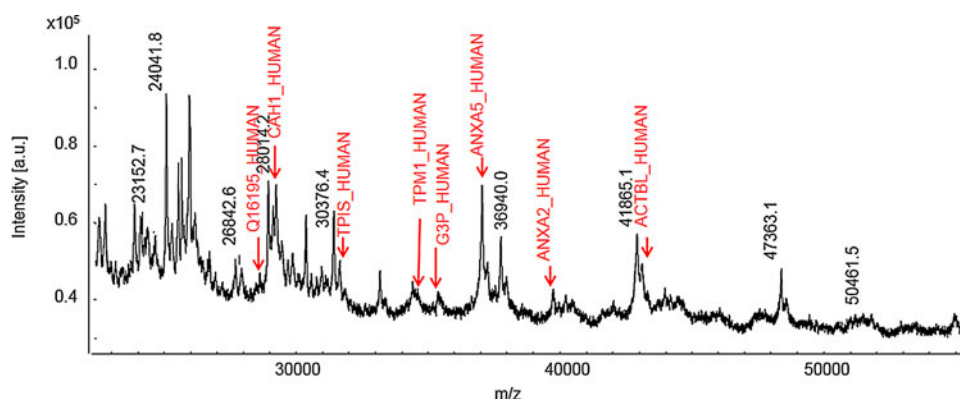AND SHOTGUN ANALYSIS (BOTTOM-UP) OR THE HFIP/2D CTAB/SDS-PAGE STRATEGY

Bottom-Up

Reference	Gene Name	MW (Da)	Score
P0C0S5	H2AZ_HUMAN	13413	232.53
P68032	ACTC_HUMAN	42019	195.24
Q00839	HNRPU_HUMAN	90584	135.69
P06899	H2B1J_HUMAN	13904	119.61
Q562R1	ACTBL_HUMAN	42003	101.48
F5H265	F5H265_HUMAN	16841	94.45
P29401	TKT_HUMAN	67878	77.75
Q14697-2	GANAB_HUMAN	106874	60.72
P07910-2	HNRPC_HUMAN	33670	58.47
Q5SSJ5	HP1B3_HUMAN	61207	58.2
Q9Y2Q3	GSTK1_HUMAN	25497	57.77
O00425	IF2B3_HUMAN	63705	56.05
E9PCY7	HNRNPH1_HUMAN	47087	54.5
Q9P2E9-2	RRBP1_HUMAN	152472	53.7
Q14152	EIF3A_HUMAN	166569	50.67
P07951	TPM2_HUMAN	32851	44.35
Q02878	RL6_HUMAN	32728	43.26
Q5T5P2	SKT_HUMAN	214116	41.34
Q9HDC9	APMAP_HUMAN	46480	40.89
D6RE83	D6RE83_HUMAN	23175	38.59
P48735	IDHP_HUMAN	50909	37.03
F8VV40	F8VV40_HUMAN	69285	35.25
P07237	PDIA1_HUMAN	57116	34.72
P42167	LAP2B_HUMAN	50670	34.71
P27816-6	MAP4_HUMAN	121005	33.19
O60716-21	CTND1_HUMAN	108170	32.85
Q9BSJ8	ESYT1_HUMAN	122856	31.78
B7Z9F1	B7Z9F1_HUMAN	55993	31.3
C9JD32	C9JD32_HUMAN	9670	31.04
P18124	RL7_HUMAN	29226	30.97
Q8NFV4	ABHDB_HUMAN	34690	30.06

HFIP/ CTAB-PAGE

Reference	Gene Name	MW (Da)	Score
P02768	ALBU_HUMAN	69367	143
P60174	TPIS_HUMAN	30791	96
P07900	HS90A_HUMAN	84660	95
Q16195	Q16195_HUMAN	27660	88
P35579	MYH9_HUMAN	226532	87
P08758	ANXA5_HUMAN	35937	70
P00915	CAH1_HUMAN	28870	70
P02647	APOA1_HUMAN	30778	70
P21333	FLNA_HUMAN	280739	67
P02545	LMNA_HUMAN	74139	67
P08670	VIME_HUMAN	53652	67
P07437	TBB5_HUMAN	49671	65
P09493	TPM1_HUMAN	32709	64
P18206	VINC_HUMAN	123799	62
P11021	GRP78_HUMAN	72333	62
P02751	FINC_HUMAN	262625	60
P12814	ACTN1_HUMAN	103058	60
P60709	ACTB_HUMAN	41737	57
P07355	ANXA2_HUMAN	38604	57
P02792	FRIL_HUMAN	20020	55
P63244	GBLP_HUMAN	35077	53
P21695	GPDA_HUMAN	37568	47
Q9H2D6	TARA_HUMAN	261376	40

Only proteins with scores >30 have been selected.

FIG. 4. String networks representations. **(A)** The protein identified after HFIP/2D CTAB/SDS-PAGE extraction and separation. The network of these hydrophobic proteins shows a tight interaction between the proteins. **(B)** The protein identified after on-tissue digestion followed by tissue extraction and shotgun analyses. The network of these proteins reflects fewer interactions between the identified proteins compared with that discovered in Figure 3.

FIG. 5. Back correlation between identified protein after 2D CTAB/SDS-PAGE separation and those detected via MALDI profiling. The mass spectrum after the HFIP high mass protein extraction procedure is annotated with the proteins that were identified after 2D gel separation.

enzyme is known to be upregulated in colorectal cancer (Bekku et al., 2000).

Discussion

The on-tissue analysis of proteins via MALDI did not allow the user to access an m/z over 30,000. To counteract the lack of the classical tissue profiling method, our group developed a procedure enabling the extraction and the detection of proteins up to 70,000 m/z (Franck et al., 2010; van Remoortere et al., 2010). This method was based on the use of the protein extraction properties of HFIP from tissue sections. After detecting these proteins via MALDI MSI or MALDI profiling, identification remains a problem. To overcome this bottleneck, we adapted the protein chemistry statements acquired from the sample preparation for 2D electrophoresis to the direct profiling analysis of tissue sections. Protein denaturation and the exposition of the hydrophobic groups to the solubilization environment are issues in sample preparation. Because the same objective was sought for this high-mass protein tissue treatment, we attempted to use the HFIP solvent for the hydrophobic protein extraction prior to 2D electrophoresis. This approach was possible due to the high compatibility of HFIP solvent with many bottom-up and -top down identification strategies.

This top-down workflow can be compared with bottom-up analyses. The methodology is illustrated in Figure 1.

We decided to use the diagonal gel electrophoresis method because it was known to give the best data for the high-mass proteome, especially via the cationic detergent cetyl-trimethyl ammonium bromide (CTAB)-PAGE (Braun et al., 2007; Polati et al., 2009; Yamaguchi et al., 2008a, b).

Using this separation method, a panel of markers for cell proliferation, cell migration and adhesion, tumor progression, and iron storage was found.

We also compared the proposed identification method with on tissue digestion of FFPE tissues and found different proteins in the highest scores.

These results suggest that extraction processes with the aqueous tryptic solution on FFPE tissue sections are wholly different than those with sinapinic acid in HFIP with fr/fr tissues. HFIP extraction is more dedicated to the less accessible proteins (such as the more hydrophobic proteins) that cannot be detected with the classical extraction methods upstream. Taken together, these data indicate that the two technologies are complementary for MALDI profiling protein identification, and it is necessary to develop on-tissue microchemistry to select specific classes of proteins such as fluorescent affinity tags (FAT) for phosphoproteins (Stevens et al., 2005).

A back correlation between identifications from CTAB/SDS-PAGE and signals obtained from tissue profiling was attempted and some proteins of the same masses were retrieved using this strategy. However, it was noteworthy that many proteins cannot be retrieved in the tissue section after analyses, meaning that many of these cannot be identified using a simple peptide mass fingerprint analysis. LC-MS analyses of the digests of each area may be performed to identify all proteins in a single location. Furthermore, it is difficult to obtain quantification information from on-tissue MALDI experiments because of the potential ion suppression effects occurring during the analysis. Further validations using classical methods, such as immuno-histochemistry, are then needed to determine the presence of the proteins in the tissue. However, based on the histological validation of the expected biomarkers, it may be possible to statistically validate the correlation between the detected m/z and the actual presence of the proteins in large patient cohorts. The combination of on-tissue analyses and 2DGE may then be a good priming workflow for the discovery of new biomarkers in tissues. After the validation of these correlations, the MALDI signature may be useful for the extemporaneous analyses of tissues in surgery blocks with the intent to obtain insight into the protein markers of cancerous tissues.

Conclusion

This strategy combining MALDI profiling with HFIP/2D CTAB/SDS-PAGE identification and on-tissue digestion, followed by shot-gun analyses, enabled us to discover proteins that are implicated in the physiopathology of ovarian tumors. These data represent another step in the enlargement of the mass range of on-tissue protein identification. Before the use of specific solvents for the extraction of proteins from tissue sections, mass range analyses were limited to less than

m/z 30,000 proteins (Franck et al., 2010; Longuespee et al., 2012a). Here, we proposed the combined use of the solvent HFIP for both the on-tissue profiling analysis and detection of higher mass proteins and the identification of these proteins with a 2D electrophoresis-based approach. Because this approach was performed using a biopsy containing both normal and cancerous tissues, this method could enable histologically based biomarker research for higher mass proteins. The chemical processes enabled the detection of proteins not detected with classical extraction procedures using the solvent mixture (ACN/TFA0.1% 70:30) classically used for sinapinic acid. The PCA-driven comparison of benign and cancerous regions of a biopsy can then enable one to highlight a panel of m/z markers specific to the cancerous region. This information assisted us in the identification of proteins from 2DE gels that were run from HFIP-extracted samples. This method could then be applied to any early stage cancer biomarkers research in an anatomical context. These combined approaches are complementary to the on-tissue digestion of proteins from FFPE tissues because they enable the identification of different groups of proteins. On-tissue bottom-up analyses of FFPE tissues may now be combined with top-down analyses on fr/fr tissue to obtain a larger view of the proteome. Thus, we have an overview of a large swathe of the proteins that differentiate between the benign and the cancerous parts of a tissue section.

The next step of such an investigation would be the validation of these proteins through classical histological approaches, such as immunohistochemistry (Sternberger et al., 1970), or newly developed methods combining classical histology and mass spectrometry such as Tag Mass (Stauber et al., 2010) or spectro-immunohistochemistry (SIHC) (Longuespee et al., 2013a).

Based on data obtained from the validation of the identified biomarkers, a statistical validation of the correlation between the detected m/z via MALDI on tissue profiling and the actual presence of the expected biomarkers may be performed. The profiling approach may then be used for the extemporaneous validation of proteomic signatures of cancerous afflictions in surgery blocs with a high confidence for the identity of the proteins.

These prospects may open new doors for personalized medicine research and development by adding a molecular dimension to extemporaneous histological analyses.

Acknowledgments

Author Disclosure Statement

References

Balluff B, Rauser S, Meding S, et al. (2011). MALDI imaging identifies prognostic seven-protein signature of novel tissue markers in intestinal-type gastric cancer. Am J Pathol 179, 2720–2729.

Bekku S, Mochizuki H, Yamamoto T, Ueno H, Takayama E, and Tadakuma T. (2000). Expression of carbonic anhydrase I or II and correlation to clinical aspects of colorectal cancer. Hepatogastroenterology 47, 998–1001.

Bonnel D, Longuespee R, Franck J, et al. (2011). Multivariate analyses for biomarkers hunting and validation through on-tissue bottom-up or in-source decay in MALDI-MSI: Application to prostate cancer. Anal Bioanal Chem 401, 149–165.

Braun RJ, Kinkl N, Beer M, and Ueffing M. (2007). Two-dimensional electrophoresis of membrane proteins. Anal Bioanal Chem 389, 1033–1045.

Calligaris D, Longuespee R, Debois D, et al., (2013). Selected protein monitoring in histological sections by targeted MALDI-FTICR in-source decay imaging. Anal Chem 85, 2117–2126.

Colinge J, Chiappe D, Lagache S, Moniatte M, and Bougueleret L. (2005). Differential proteomics via probabilistic peptide identification scores. Anal Chem 77, 596–606.

Deininger SO, Ebert MP, Futterer A, Gerhard M, and Rocken C. (2008). MALDI imaging combined with hierarchical clustering as a new tool for the interpretation of complex human cancers. J Proteome Res 7, 5230–5236.

Di Michele M, Marcone S, Cicchillitti L, et al. (2010). Glycoproteomics of paclitaxel resistance in human epithelial ovarian cancer cell lines: Towards the identification of putative biomarkers. J Proteomics 73, 879–898.

Dong HP, Holth A, Kleinberg L, et al. (2009). Evaluation of cell surface expression of phosphatidylserine in ovarian carcinoma effusions using the annexin-V/7-AAD assay: Clinical relevance and comparison with other apoptosis parameters. Am J Clin Pathol 132, 756–762.

El Ayed M, Bonnel D, Longuespee R, et al. (2010). MALDI imaging mass spectrometry in ovarian cancer for tracking, identifying, and validating biomarkers. Med Sci Monit 16, BR233–245.

Elsner M, Rauser S, Maier S, et al. (2012). MALDI imaging mass spectrometry reveals COX7A2, TAGLN2 and S100-A10 as novel prognostic markers in Barrett's adenocarcinoma. J Proteomics 75, 4693–4704.

Franck J, Longuespee R, Wisztorski M, et al. (2010). MALDI mass spectrometry imaging of proteins exceeding 30,000 daltons. Med Sci Monit 16, BR293–299.

Gagnon H, Franck J, Wisztorski M, Day R, Fournier I, and Salzet M. (2012). Targeted mass spectrometry imaging: Specific targeting mass spectrometry imaging technologies from history to perspective. Prog Histochem Cytochem 47, 133–174.

Iwanicki MP, Davidowitz RA, Ng MR, et al. (2012). Ovarian cancer spheroids use myosin-generated force to clear the mesothelium. Cancer Discov 1, 144–157.

Lemaire R, Desmons A, Tabet JC, Day R, Salzet M, and Fournier I. (2007). Direct analysis and MALDI imaging of formalin-fixed, paraffin-embedded tissue sections. J Proteome Res 6, 1295–1305.

Lemaire R, Wisztorski M, Desmons A, et al. (2006). MALDI-MS direct tissue analysis of proteins: Improving signal sensitivity using organic treatments. Anal Chem 78, 7145–7153.

Lokman NA, Ween MP, Oehler MK, and Ricciardelli C. (2011). The role of annexin A2 in tumorigenesis and cancer progression. Cancer Microenviron 4, 199–208.

Longuespee R, Boyon C, Castellier C, et al. (2012a). The C-terminal fragment of the immunoproteasome PA28S (Reg alpha) as an early diagnosis and tumor-relapse biomarker: Evidence from mass spectrometry profiling. Histochem Cell Biol 138, 141–154.

Longuespee R, Boyon C, Desmons A, et al. (2013a). Spectro-immunohistochemistry: A novel form of MALDI mass spectrometry imaging coupled to immunohistochemistry for tracking antibodies. Omics 2, 132–141.

Longuespee R, Boyon C, Desmons A, et al. (2012b). Ovarian cancer molecular pathology. Cancer Metastasis Rev 31, 713–732.

Longuespee R, Gagnon H, Boyon C, et al. (2013b). Proteomic analyses of serous and endometrioid epithelial ovarian cancers—Cases studies—Molecular insights of a possible histological etiology of serous ovarian cancer. Proteomics Clin Appl 7, 337–354.

Lyubimova T, Caglio S, Gelfi C, Righetti PG, and Rabilloud T. (1993). Photopolymerization of polyacrylamide gels with methylene blue. Electrophoresis 14, 40–50.

Maier SK, Hahne H, Moghaddas Gholami A, et al. (2013). Comprehensive identification of proteins from MALDI imaging. Mol Cell Proteomics 12, 2901–2910.

Meding S, Balluff B, Elsner M, et al. (2012). Tissue-based proteomics reveals FXYD3, S100A11 and GSTM3 as novel markers for regional lymph node metastasis in colon cancer. J Pathol doi: 10.1002/path.4021 [Epub ahead of print].

Nanduri B, Lawrence ML, Vanguri S, Pechan T, and Burgess SC. (2005). Proteomic analysis using an unfinished bacterial genome: The effects of subminimum inhibitory concentrations of antibiotics on Mannheimia haemolytica virulence factor expression. Proteomics 5, 4852–4863.

Pocsfalvi G, Votta G, De Vincenzo A, et al. (2011). Analysis of secretome changes uncovers an autocrine/paracrine component in the modulation of cell proliferation and motility by c-Myc. J Proteome Res 10, 5326–5337.

Polati R, Zapparoli G, Giudici P, and Bossi A. (2009). A CTAB based method for the preparation of total protein extract of wine spoilage microrganisms for proteomic analysis. J Chromatog B, Anal Technol Biomed Life Sci 877, 887–891.

Prokocimer M, Davidovich M, Nissim-Rafinia M, et al. (2009). Nuclear lamins: Key regulators of nuclear structure and activities. J Cell Mol Med 13, 1059–1085.

Quanico J, Franck J, Dauly C, et al. (2013). Development of liquid microjunction extraction strategy for improving protein identification from tissue sections. J Proteomics 79, 200–218.

Rao LV, Tait JF, and Hoang AD. (1992). Binding of annexin V to a human ovarian carcinoma cell line (OC-2008). Contrasting effects on cell surface factor VIIa/tissue factor activity and prothrombinase activity. Thromb Res 67, 517–531.

Stauber J, Ayed ME, Wisztorski M, Salzet M, and Fournier I. (2010). Specific MALDI-MSI: Tag-Mass. Methods Mol Biol 656, 339–361.

Stauber J, Lemaire R, Franck J, et al. (2008). MALDI imaging of formalin-fixed paraffin-embedded tissues: Application to model animals of Parkinson disease for biomarker hunting. J Proteome Res 7, 969–978.

Sternberger LA, Hardy PH, Jr., Cuculis JJ, and Meyer HG. (1970). The unlabeled antibody enzyme method of immuno-histochemistry: Preparation and properties of soluble antigen-antibody complex (horseradish peroxidase-antihorseradish peroxidase) and its use in identification of spirochetes. J Histochem Cytochem 18, 315–333.

Stevens SM, Jr., Chung AY, Chow MC, et al. (2005). Enhancement of phosphoprotein analysis using a fluorescent affinity tag and mass spectrometry. Rapid Commun Mass Spectrom 19, 2157–2162.

Sugimura M, Donato R, Kakkar VV, and Scully MF. (1994). Annexin V as a probe of the contribution of anionic phospholipids to the procoagulant activity of tumour cell surfaces. Blood Coagul Fibrinolysis 5, 365–373.

Van Remoortere A, Van Zeijl RJ, Van Den Oever N, Fet al. (2010). MALDI imaging and profiling MS of higher mass proteins from tissue. J Am Soc Mass Spectrom 21, 1922–1929.

Wisztorski M, Fatou B, Franck J, et al. (2013). Microproteomics by liquid extraction surface analysis: Application to FFPE tissue to study the fimbria region of tubo-ovarian cancer. Proteomics Clin Appl 7, 234–240.

Xue LY, Teng LH, Zou SM, et al. (2007). [Expression of annexin I in different histological types of carcinomas]. Zhonghua Zhong Liu Za Zhi 29, 444–448.

Yamaguchi Y, Miyagi Y, and Baba H. (2008a). Two-dimensional electrophoresis with cationic detergents, a powerful tool for the proteomic analysis of myelin proteins. Part 1: Technical aspects of electrophoresis. J Neurosci Res 86, 755–765.

Yamaguchi Y, Miyagi Y, and Baba H. (2008b). Two-dimensional electrophoresis with cationic detergents, a powerful tool for the proteomic analysis of myelin proteins. Part 2: Analytical aspects. J Neurosci Res 86, 766–775.

Address correspondence to:
Dr. Isabelle Fournier
Laboratoire PRISM
Universite de Lille 1
Bâtiment SN3 1ᵉ étage
Avenue Paul Langevin
Villeneuve D'Ascq 59650
France

E-mail: isabelle.fournier@univ-lille1.fr

or

Dr. Michel Salzet
Laboratoire PRISM
Universite de Lille 1
Bâtiment SN3 1ᵉ étage
Avenue Paul Langevin
Villeneuve D'Ascq 59650
France

E-mail: michel.salzet@univ-lille1.fr